33rd Annual International Conference of the IEEE EMBS
Boston, Massachusetts USA, August 30 - September 3, 2011

In-cycle Myocardium Tissue Electrical Impedance Monitoring Using Broadband Impedance Spectroscopy

Benjamin Sanchez, Gerd Vandersteen, Javier Rosell-Ferrer, Joan Cinca and Ramon Bragos

Abstract— **Measurements of myocardium tissue impedance during the cardiac cycle have information about the morphology of myocardium cells as well as cell membranes and intra/extra cellular spaces. Although the variation with time of the impedance cardiac signal has information about the myocardium tissue activity during the cardiac cycle, this information has been usually underestimated in the studies based on frequency-sweep Electrical Impedance Spectroscopy (EIS) technique. In these cases, the dynamic behavior was removed from the impedance by means of averaging. The originality of this research is to show the time evolution of *in-vivo* healthy myocardium tissue impedance during the cardiac cycle, being measured with a multisine excitation at 26 frequencies (1 kHz - 1 MHz). The obtained parameters from fitting data to a Cole model are valid indicators to explain the time relation of the systolic and diastolic function with respect to the myocardium impedance time variation. This paper presents a successful application of broadband Impedance Spectroscopy for time-varying impedance monitoring. Furthermore, it can be extended to understand various unsolved problems in a wide range of biomedical and electrochemical applications, where the system dynamics are intended to be studied.**

I. Introduction

Myocardial electrical impedance holds promise in detecting different tissue states. Through animal *in-vivo* and *ex-vivo* tissue experiments, it has been shown to correlate with many physiological states of the myocardium tissue such as the regional and global ischemia processes [1], edema [2], and detect humoral rejection episodes following heart transplantation [3] and [4]. Electrical impedance characterization of myocardium tissue is usually performed at a single frequency, in the 1 kHz - 10 kHz range [5] or performing a frequency sweep in the 1 kHz - 1 MHz range [6] and [1]. The frequency sweep method has accuracy problems when measuring organs that change with time, being the heart the worst case, given that it shows abrupt changes during the cardiac cycle. The main drawback of the frequency sweep technique is its measuring time, which is much slower than the period of the impedance modulation associated with the system dynamics. Then, the modulation is under sampled and this results in noise at the measurements, which can be reduced by averaging successive sweeps. However, averaging increases the measuring time and leads to lose the potentially useful information included in the movement.

To acquire a modulation-free myocardium impedance spectrum and to determine the cardiac cycle impedance time variation is then necessary to use a broadband excitation. Such kinds of signals are able to obtain the impedance spectrum at different frequencies simultaneously, resulting in a short acquisition time if they are compared with the heart contraction rise time. To our knowledge, the first trial for characterizing the myocardium tissue impedance during the cardiac cycle was presented in 2001 [7]. The acquisition system, based on an Arbitrary Waveform Generator (12 bit D/A, 40 Msamples/s) and a digital oscilloscope (500 Msamples/s, 8 bit). In this case, the system performance was not able to measure and to process the data in real-time because of the limited memory available and the transmission time required for transmitting data through an IEEE-488 interface. As a result, the system was able to measure only 6 impedance spectrums per second during 1 second maximum. Moreover, the limited resolution at high frequency did not allow determining whether there was a spectrum change into the cycle or just a global impedance shift. Nevertheless, we continued using the frequency sweep technique for the following years and after a second attempt using a FPGA based custom system, we have developed a PXI based modular impedance analyzer that overcomes all the mentioned limitations with the objective to perform time varying tissue characterization for tissue engineering applied to myocardium regeneration.

With the aim to foresee the dynamic properties of the regenerated cardiomyocyte tissue, we measure healthy myocardium tissue during the cardiac cycle. This can contribute to improve the models of the passive properties of cardiomyocytes including its dynamic behavior.

II. Material and Methods

A. Experimental model

Commercial female swine (40 to 50 Kg) were sedated with azaperone (8 mg/Kg intramuscular, Stressnil) and anesthetized with sodium thiopental (10 mg/kg, Pentothal). After endotracheal intubation, anesthesia was maintained with isofluorane inhalation anaesthesia (1.5-2.5 vol % in O_2) with mechanical ventilation at a ventilation rate of 15 breaths/min. A midline sternotomy was performed and the heart was exposed by a pericardial cradle. Myocardial impedance was

This work has been supported in part by the Spanish Ministry MICINN SAF2008-05144-C02-02, 080331 from Fundació La Marató de TV3, by the REDINSCOR, by the Fund for Scientific Research (FWO-Vlaanderen), by the Flemish Government (Methusalem), and by the Belgian Government through the Interuniversity Poles of Attraction (IAP VI/4) Program.

The authors would like to thank E. Jorge for her helpful contribution to the animal experimentation.

J. Cinca is with the Cardiology Unit from the Hospital Santa Creu i Sant Pau (HSCSP), Barcelona, 08025, SPAIN.

G. Vandersteen is with the ELEC Department, Vrije Universiteit Brussels (VUB), Brussels, 1050, BELGIUM.

B. Sanchez, J.Rosell and R.Bragos are with the Department of Electrical Engineering, Technical University of Catalonia (UPC), Barcelona, 08034, SPAIN. benjamin.sanchez@upc.edu

measured with a four-electrode (5 mm long, 0.4 mm diameter) platinum - iridium intramural probes mounted as a linear array separated by an interelectrode distance of 1.27 mm. This interelectrode separation is small enough to ensure that the low resistivity intracavitary blood does not affect the impedance measurement. Myocardial tissue impedance was measured using a four-electrode array to reduce the electrode-tissue interface impedance.

B. Materials

Data were obtained using a custom multifrequency impedance analyzer built based on a PXI system from National Instruments. The system includes an embedded dual-core controller PXIe-8130, a 2 channel high-speed digitizer card PXIe-5122 (100 Ms/s, 64 MB/channel, 14 bits) and an Arbitrary Waveform Generator (AWG) PXI-5422 (200 Ms/s, 32 MB, 16 bits). The impedance measurements were obtained after exciting the myocardium with a four periods of a periodic multisine signal of 1 ms through a custom 4 wire Front End (FE). The measured voltage was buffered with two wideband operational amplifiers with high input impedance (AD8066) and then amplified with a selectable gain wideband instrumentation amplifier (AD8274). Current was converted to voltage with an operational amplifier with transimpedance topology (AD8066). Both acquired signals were low-pass filtered before digitizing (cutoff frequency of 10 MHz) and then digitized at 20 MHz sample rate. The FE has a Common Mode Rejection Ratio (CMRR) of 70 dB at 1 kHz and 63 dB at 1 MHz. Above 1 MHz, CMRR decreases being 45 dB at 10 MHz. The FE linearity has been determined measuring resistors from 100 Ω to 1k1 Ω. The linearity error in any case is at least the same as the tolerance of the resistors measured (1 %). The absolute linearity error at measurement frequencies between 1 kHz to 1 MHz is between 0.1 Ω and 0.4 Ω. A three-reference calibration method was employed to correct the load dependent errors [8]. Three saline solutions of known conductivity were used to determine a set of coefficients at each exciting frequency. The three references were obtained using the same probe so that the effects of electrodes, cables and the amplifier response on the measurement error were reduced. The frequency range measured was chosen from 1 kHz to 1 MHz, because measurement errors may occur both below 1 kHz, due to tissue - electrode interface impedance, and above 1 MHz, due to cable effects. Previous results [1] show that this frequency range includes the main impedance changes in the myocardium tissue.

Data acquisition was done with a customized application implemented in LabView. The application synchronizes the AWG and the digitizer and process data on-the-fly. The impedance spectrum is estimated in real-time using the Local Polynomial Method (LPM) described in [9] and [10]. A fast LPM version achieves a reduction in processing time by taking advantage of the multisine periodicity [11]. In contrast to spectral analysis based on cross and auto power spectrum, the LPM removes more efficiently the effect of the transient than the windowed spectral analysis.

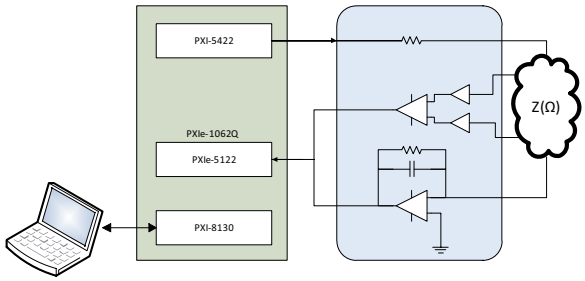

Fig. 1. Block diagram of the multifrequency impedance analyzer connected to the Front End and the biological system under test.

III. Results

Myocardial tissue impedance shown in Fig.2 was measured at three healthy animals. Fig.3 shows the myocardium impedance spectrum changes in time during a 90 seconds and measured with a four-wire impedance measurement topology using the electrodes probe described in section II-A. Electrodes were sutured to the epicardium trying to maintain the same position to minimize the movement during the measurements due to the heart contraction.

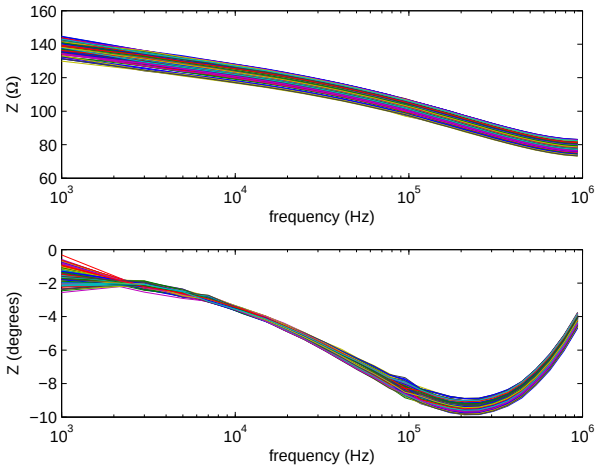

Fig. 2. Healthy myocardium impedance spectrum magnitude (top) and phase (bottom) (animal model 1).

For an homogeneous and isotropic object, the impedance can be related to its electrical properties, conductivity $\sigma\left(Sm^{-1}\right)$ and relative permittivity e_r, according to the following expression:

$$Z(\omega) = \rho^*(\omega)\frac{L}{S} = \frac{1}{\sigma^*(\omega)}\frac{L}{S} = \frac{1}{\sigma(\omega) + j\omega\varepsilon_0\varepsilon_r(\omega)}k \quad (1)$$

where $\rho^*(\Omega m)$ is the complex resistivity, $\sigma^*\left(Sm^{-1}\right)$ is the complex conductivity, ε_r is the vacuum permittivity and $k\left(m^{-1}\right)$ is known as cell factor. The cell factor k, which depends on the geometry of the electrodes $\frac{L}{S}$ and the object, was determined by measuring the impedance of physiological saline solution at 25 ^oC using the same four-electrode needles and measurement equipment that was used

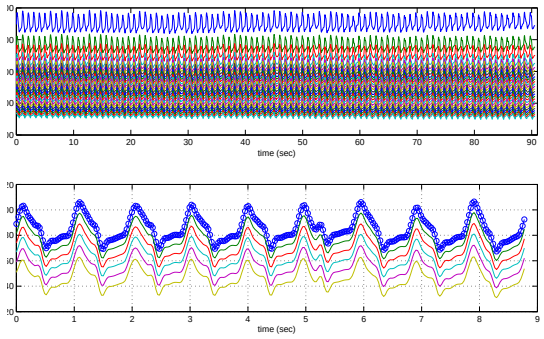

Fig. 3. Complete myocardium tissue impedance variation record during 90 seconds (top) and a zoom from 0 to 9 seconds (bottom); the impedance spectrum time resolution is 22 impedance spectra/second (animal model 2).

for the *in situ* studies. Considering the cell factor k as a constant is only valid for homogeneous and isotropic objects. Although the myocardium tissue has a strong anisotropy due to the complex structure of the fiber orientation across the myocardium wall, studies have proof that an interelectrode distance larger than the dimensions of the myocardium fibers allows to avoid the effects of the myocardium fibers direction and the measurement is an average of the impedance in both directions [1]. Thus, the estimated myocardium conductivity σ (top) and permittivity e_r (bottom) shown in Fig.4 have a limited accuracy.

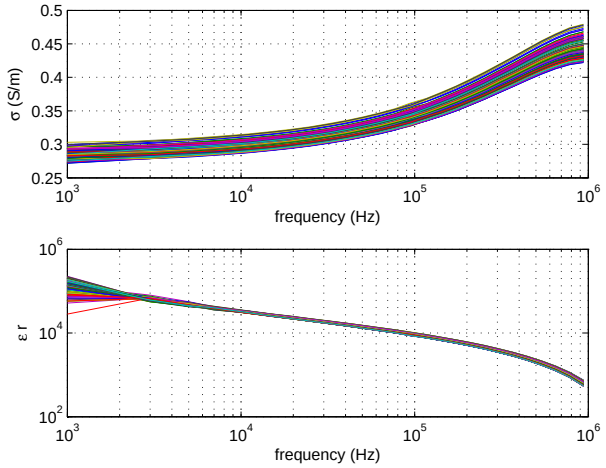

Fig. 4. Healthy myocardium tissue dielectric properties, conductivity (top) and relative permittivity (bottom) (animal model 1).

A. Data analysis

There are many different models of concentrated parameters in order to represent electrically a biological system, from a single cell to more complex systems like organs. From all the large number of empirical relaxation functions, the Cole-Cole equation [12] function for the permittivity has probably been the most widely used. The Cole-Cole equation introduces the concept of distributed time constant for more accurate representations of the impedance spectrum, which introduces the α parameter on the following equation:

$$\varepsilon^*(\omega) = \varepsilon_\infty + \frac{\varepsilon_s - \varepsilon_\infty}{1 + (j\omega\tau)^{1-\alpha}} - j\frac{\sigma_s}{\omega\varepsilon_0} \tag{2}$$

where α is an empirical parameter characteristic of the distribution of the relaxation frequencies. It is possible to rewrite the Cole-Cole equation that models the complex permittivity shown in Eq.2 considering the electrical impedance given by:

$$Z(f) = R_\infty + \frac{R_0 - R_\infty}{1 + \left(j\frac{f}{f_c}\right)^\alpha} \tag{3}$$

where the central frequency f_c is the frequency corresponding to the mean value of the distribution of the relaxation frequencies. The Eq.3 is known as Cole equation and plots an arc of circumference in the complex plane, where R_0 and R_∞ represent the intersection points of the arc over the x-axis at very low and very high frequency. The depression of center of the arc is defined by means of the α parameter. The impedance data plotted from Cole equation into the complex plane is usually referenced in the literature as Cole plot. The Cole plot represented in Fig.5 was obtained after fitting impedance data shown in Fig.2 to the Cole equation given by the Eq.3. The upper bound for the mean square error due to the fitting process was 2%. In Fig.5 it is possible to observe how the impedance changes with time, moving the Cole arc across the real axis.

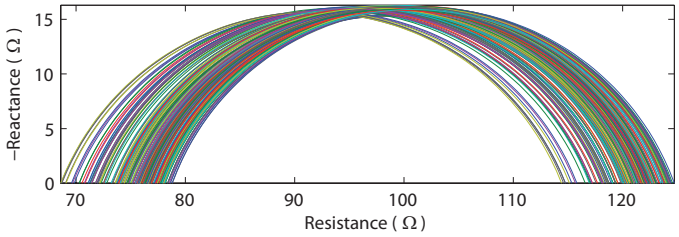

Fig. 5. Cole plot time evolution (animal model 1).

The Cole equation parameters R_0 and R_∞ time evolution are depicted in Fig.6. As it can be observed, the time modulation trend is the same for both parameters. A reasonable explanation about the relation between of R_0 and R_∞ shown in Fig.6 with respect to the α and f_c time variation is shown in Fig.7 and Fig.8 respectively. While the heart is in systole the myocardium cells are contracted and this is reflected as a decrease of the α parameter. At the same time, the central frequency f_c of the impedance relaxation increases due to that the myocardium cells are smaller. During the diastole, the myocardium cells are expanded and this morphological change is translated into a larger myocardium cells with lower central frequency f_c of the impedance relaxation. In this case, there is a wide cell's dimension variety, which is modeled in the Cole-Cole equation as a higher time constant dispersion, reflected into an increase of the α parameter in the Cole equation.

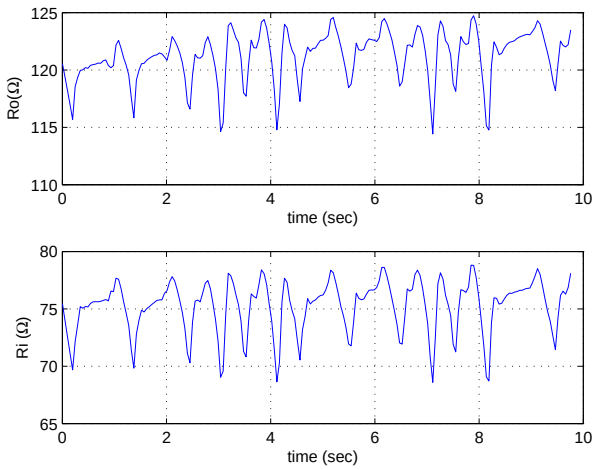

Fig. 6. Cole model parameters R_0 (top) and R_i (bottom) time evolution (animal model 1).

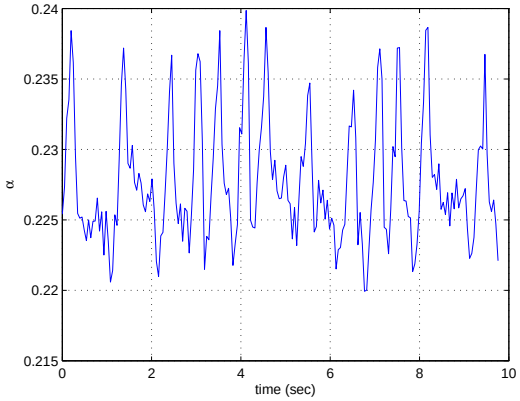

Fig. 7. α Cole model parameter time evolution (animal model 1).

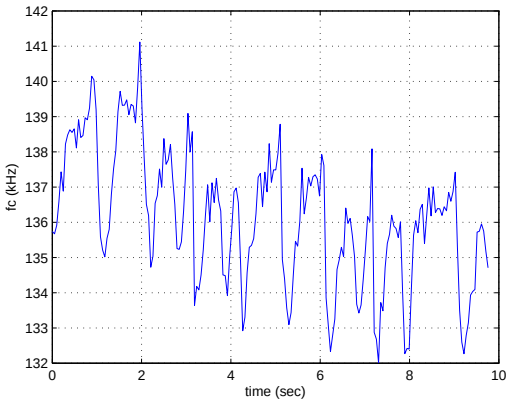

Fig. 8. Central frequency f_c Cole model parameter time evolution (animal model 1).

IV. Conclusions

The results obtained agree with the expected effect of the myocyte contraction to the myocardium impedance relaxation. Based on the results of the present study, it seems feasible to detect how the systolic and diastolic function change during an ischemia by means of impedance monitoring. Current work includes measuring the myocardium tissue impedance after an occlusion of the Left Anterior Descending (LAD) coronary artery below-the first diagonal branch. The evolving changes of the myocardium fibers contractility with time will be studied during the ischemic process. Simultaneous acquisition of pressure wave in the ventricle and its correlation with the Cole parameters will help to interpret the results.

References

[1] Y. Salazar, R. Bragos, O. Casas, J. Cinca, and J. Rosell *Transmural versus nontransmural in situ electrical impedance spectrum for healthy, ischemic, and healed myocardium,* vol. 51, no. 8, (*IEEE Trans Biomed Eng,*) pp. 1421–1427, Aug 2004.

[2] M. M. Gebhard, E. Gersing, and C. J. Brockhoff et al. *Impedance spectroscopy: a method for surveillance of ischemia tolerance of the heart,* vol. 35, (*Thorac. Cardiovasc. Surgeon,*) pp. 26–32, 1987.

[3] O. Grauhan, J. Muller, C. Knosalla, T. Cohnert, H. Siniawski, H. D.Volk E. Fietze, W. Kupetz, and R. Hetzer *Electric myocardial impedance registration in humoral rejection after heart transplantation,* vol. 15, (*J. Heart Lung Transplant*) pp. 136–143, 1996.

[4] J. Cinca, J. Ramos, M. A. Garcia, R. Bragos, A. Bayes, Y. Salazar, R. Bordes, S. Mirabet, J. M. Padro, J. G. Picart, X. Violas, and J. Rosell *Changes in myocardial electrical impedance in human heart graft rejection,* vol. 10, no. 6, (*Eur J Heart Fail*) pp. 594–600, Jun 2008.

[5] M. A. Fallert, M. S. Mirotznik, S. W. Downing, E. B. Savage, K. R. Foster, M. E. Josephson and D. K. Bogen *Myocardial electrical impedance mapping of ischemic sheep hearts and healing aneurysms,* vol. 87, (*Circulation*) pp. 199-207, 1993.

[6] E. Gersing *Measurement of electrical impedance in organs - measuring equipment for research and clinical applications,* vol. 36, no. 1-2, (*BiomedizinischeTechnik*) pp. 6–1, Jan 1991.

[7] R. Bragos, R. Blanco-Enrich, O. Casas and J. Rosell *Characterisation of dynamic biologic systems using multisine based impedance spectroscopy,* no. 1, (*IEEE Proceedings on Instrumentation and Measurement Technology Conference*) pp. 44–47, 2001.

[8] J.Z. Bao, C.C Davis and R.E. Schmukler *Impedance spectroscopy of human erythrocytes: system calibration and nonlinear modeling,* vol. 40, no. 4 (*IEEE transactions on Biomedical Engineering,*) pp. 364–378, 1993.

[9] R. Pintelon, J.Schoukens, G.Vandersteen and K.Barbe *Estimation of non parametric noise and FRF models for multivariable systems PartI:Theory,* (*Journal of Mechanical Systems and Signal Processing,*) 2009.

[10] R. Pintelon, G.Vandersteen, J.Schoukens and Y.Rolain *Improved (non-) parametric identification of dynamic systems excited by periodic signals The multivariate case,* (*Journal of Mechanical Systems and Signal Processing,*) 2011.

[11] B. Sanchez, J.Schoukens, R.Bragos and G.Vandersteen, *Novel Estimation of the Electrical Bioimpedance using the Local Polynomial Method. Application to In-cycle Myocardium Tissue Impedance Characterization,*submitted.

[12] K. S. Cole *Dispersion and absorption in dielectrics i. alternating current characteristics,* vol. 9, (*Journal of Chemical Physics,*) pp. 341-351, 1941.